

# Optically Modulated High-Sensitivity Heterostructure Varactor

Xia Zhao, Adriano Cola, Andrea Tersigni, Fabio Quaranta, Eric Gallo, Jonathan E. Spanier, and Bahram Nabet, *Member, IEEE*

**Abstract**—A novel optically modulated high-sensitivity heterostructure varactor, demonstrated as a strong candidate for high-order frequency-multiplier applications, is reported. The device is a  $\delta$  modulation-doped heterostructure of AlGaAs/GaAs with two Schottky contacts on the top. The capacitance–voltage ( $C$ – $V$ ) measurements show a  $C_{\max}/C_{\min}$  ratio up to 113 and an extremely high nonlinearity during the transition from high to low capacitance with sensitivity of up to 35. These results are one of the best obtained so far among similar structure devices. In addition, optoelectronic experimental results demonstrate that the slope of the  $C$ – $V$  relationship can be modulated by the intensity of the incident optical power. A model describing the source of the reported  $C$ – $V$  results is proposed along with the simulation results verifying the observed  $C$ – $V$  behavior.

**Index Terms**—Frequency multiplier, heterostructure-barrier-varactor (HBV), metal–semiconductor–metal (MSM), optical modulation, two-dimensional-hole-gas (2-DHG).

## I. INTRODUCTION

VARACTORS have been widely applied in parametric amplifiers and various frequency converting circuits [1], voltage-controlled oscillator (VCOs), and tuned matching networks [2]. Most of the applications seek large  $C_{\max}/C_{\min}$  ratios and a high-quality factor  $Q_c$ . However, applications such as high-order frequency multipliers by odd harmonic generations create a strong demand on high nonlinearity of capacitance–voltage ( $C$ – $V$ ) characteristics is created. Previously, Schottky diodes [3] have been used for this purpose, however, heterostructure-barrier-varactors (HBV) offer the potential for a better overall performance in terms of conversion efficiency and operation frequency due to their power handling capabilities and their symmetric  $C$ – $V$  relation, which circumvents the idler and bias circuits in a multiplier. The first HBV was reported in 1989 [4], thereafter, a number of frequency triplers [5], [6] and quintuplers [7] have been reported based on this structure. More recently, heterostructures combined with Schottky contacts, such as metal–semiconductor–metal

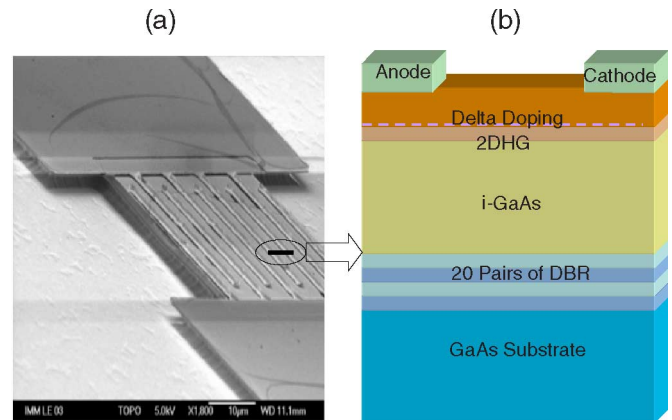


Fig. 1. (a) Side-view SEM picture of the device. (b) Cross section of the device between two fingers.

(MSM)–two-dimensional electron gas (2-DEG) [8] and gate-controlled Schottky/2-DEG varactors [9], have also been reported exhibiting excellent electrical properties.

In this letter, we report on the fabrication of a varactor with a Schottky MSM heterostructure 2-D-hole-gas (2-DHG) and distributed-Bragg-reflectors (DBR) for optical enhancement. Compared to the previous 2-DEG devices, the charge distributions in the  $\delta$ -doped layer and the absorption region are different, which eventually results in a higher sensitivity of the  $C$ – $V$ . The improved electrical and optical performances of these devices are discussed. The devices demonstrate high nonlinearity and very low leakage current, allowing for high power conversion efficiency in frequency-multiplier applications. Moreover, since the device was designed as a photodetector, optoelectronic experiments show that the nonlinear  $C$ – $V$  characteristics can be controlled by the intensity of the optical radiation, offering the potential for applications in optoelectronic mixing in monolithic microwave integrated circuit (MMIC) and RF circuits [10], given that the planar MSM structure allows them to be monolithically integrated into III–V technology.

## II. DEVICE STRUCTURE, FABRICATION, AND PERFORMANCE

The device consists of two Schottky contacts on the top of a  $\delta$ -layer modulation-doped AlGaAs/GaAs heterostructure. The wafer for the device fabrication was grown by molecular beam epitaxy (MBE) on a (100)-oriented semi-insulating GaAs substrate. The SEM image and the schematics of the device are shown in Fig. 1. An SEM side-view image of a mesa isolated

Manuscript received March 30, 2006; revised June 6, 2006. The work of J. E. Spanier was supported in part by the U. S. Army Research Office under Award W911NF-04-1-0308. The work of B. Nabet was supported by the National Science Foundation under Award ECS 01107073. The review of this letter was arranged by Editor T. Mizutani.

X. Zhao, E. Gallo, J. E. Spanier, and B. Nabet are with the Electrical and Computer Engineering Department, Drexel University, Philadelphia, PA 19104 USA.

A. Cola, A. Tersigni, and F. Quaranta are with the Consiglio Nazionale delle Ricerche (CNR)/Istituto per la Microelettronica ed i Microsistemi (IMM) Sezione di Lecce, 73100 Lecce, Italy.

Color versions of all figures are available online at <http://ieeexplore.ieee.org>. Digital Object Identifier 10.1109/LED.2006.880637

Report Documentation Page			Form Approved OMB No. 0704-0188		
Public reporting burden for the collection of information is estimated to average 1 hour per response, including the time for reviewing instructions, searching existing data sources, gathering and maintaining the data needed, and completing and reviewing the collection of information. Send comments regarding this burden estimate or any other aspect of this collection of information, including suggestions for reducing this burden, to Washington Headquarters Services, Directorate for Information Operations and Reports, 1215 Jefferson Davis Highway, Suite 1204, Arlington VA 22202-4302. Respondents should be aware that notwithstanding any other provision of law, no person shall be subject to a penalty for failing to comply with a collection of information if it does not display a currently valid OMB control number.					
1. REPORT DATE <b>SEP 2006</b>		2. REPORT TYPE		3. DATES COVERED <b>00-00-2006 to 00-00-2006</b>	
4. TITLE AND SUBTITLE <b>Optically Modulated High-Sensitivity Heterostructure Varactor</b>			5a. CONTRACT NUMBER		
			5b. GRANT NUMBER		
			5c. PROGRAM ELEMENT NUMBER		
6. AUTHOR(S)			5d. PROJECT NUMBER		
			5e. TASK NUMBER		
			5f. WORK UNIT NUMBER		
7. PERFORMING ORGANIZATION NAME(S) AND ADDRESS(ES) <b>Drexel University, Department of Electrical and Computer Engineering, Philadelphia, PA, 19104</b>			8. PERFORMING ORGANIZATION REPORT NUMBER		
9. SPONSORING/MONITORING AGENCY NAME(S) AND ADDRESS(ES)			10. SPONSOR/MONITOR'S ACRONYM(S)		
			11. SPONSOR/MONITOR'S REPORT NUMBER(S)		
12. DISTRIBUTION/AVAILABILITY STATEMENT <b>Approved for public release; distribution unlimited</b>					
13. SUPPLEMENTARY NOTES					
14. ABSTRACT <b>A novel optically modulated high-sensitivity heterostructure varactor, demonstrated as a strong candidate for high-order frequency-multiplier applications, is reported. The device is a modulation-doped heterostructure of AlGaAs/GaAs with two Schottky contacts on the top. The capacitance?voltage (C?V ) measurements show a Cmax/Cmin ratio up to 113 and an extremely high nonlinearity during the transition from high to low capacitance with sensitivity of up to 35. These results are one of the best obtained so far among similar structure devices. In addition, optoelectronic experimental results demonstrate that the slope of the C?V relationship can be modulated by the intensity of the incident optical power. A model describing the source of the reported C?V results is proposed along with the simulation results verifying the observed C?V behavior.</b>					
15. SUBJECT TERMS					
16. SECURITY CLASSIFICATION OF:			17. LIMITATION OF ABSTRACT <b>Same as Report (SAR)</b>	18. NUMBER OF PAGES <b>3</b>	19a. NAME OF RESPONSIBLE PERSON
a. REPORT <b>unclassified</b>	b. ABSTRACT <b>unclassified</b>	c. THIS PAGE <b>unclassified</b>			

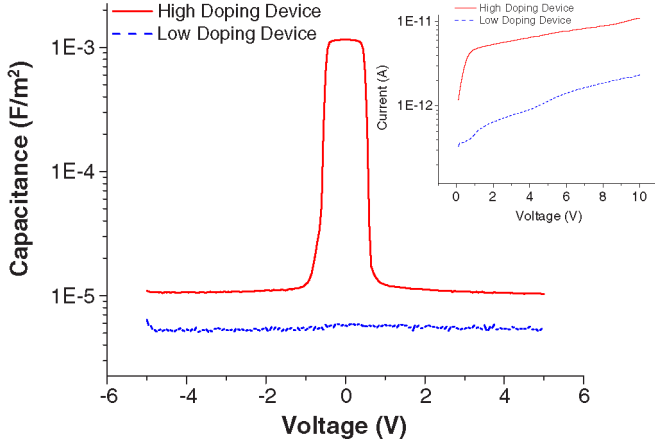


Fig. 2.  $C$ - $V$  characteristics of the high and low-doped devices in the dark at probe frequency of 10 kHz. Inset is the current-voltage characteristics.

fabricated device is shown in Fig. 1(a), illustrating interdigitated fingers. The growth layer structure is shown in Fig. 1(b) and was verified by the SEM cross-sectional image. The  $\text{Al}_{0.9}\text{Ga}_{0.1}\text{As}/\text{Al}_{0.24}\text{Ga}_{0.76}\text{As}$  DBRs, with thickness of 67.6 and 59.6 nm, respectively, for the purpose of enhancing optical reflection, were grown on the GaAs buffer followed by a GaAs absorption layer 117.5-nm thick with the  $\text{Al}_{0.5}\text{Ga}_{0.5}\text{As}$  barrier enhancement layer 50-nm thick above it. An Al-component of 0.5 was designed to increase the valence-band offset up to 0.21 eV [11] for better confinement of the hole gas. A Be atomic-planar-doping (APD) in the barrier enhancement layer is 7-nm away from the  $\text{AlGaAs}/\text{GaAs}$  heterointerface with a nominal density of  $2.5 \times 10^{12}/\text{cm}^2$ . This  $\delta$ -modulation-doped heterostructure creates a 2-DHG along the heterojunction. The device was fabricated following standard procedures, including optical lithography, metal evaporation, and lift off. The interdigitated electrodes were deposited with a Ti/Pt/Au multilayer, forming Schottky contacts to the semiconductor. The area of each electrode is  $200 \times 80 \mu\text{m}^2$ , and the device area is  $40 \times 40 \mu\text{m}^2$  with the number of fingers varying for different electrode geometries.

$C$ - $V$  measurements on the device were performed with an HP4284A precision LCR meter. The capacitances of the device were obtained by subtracting the stray capacitance contributions. Identical devices were fabricated with a  $\delta$ -doping level of  $5 \times 10^{11}/\text{cm}^2$  to investigate the effect of the  $\delta$ -doping. The measured  $C$ - $V$  behavior of the devices is shown in Fig. 2. We observe significant differences between the high doped (HD) and low doped (LD) devices. The capacitance of the HD device has a peak of 2 pF and remains flat until about 0.7 V, then sharply drops to a relatively low value of less than 0.02 pF, varying upon the electrode geometries. The ratio of  $C_{\text{max}}/C_{\text{min}}$  at a probe frequency of 10 kHz was measured up to 113 for a no-finger device. The best results previously reported was around 100 [7]. Given this  $C$ - $V$  behavior, the sheet carrier density is estimated to be  $5.5 \times 10^{11}/\text{cm}^2$  using the charge control model, thus a giving series resistance of around 100  $\Omega$  and a dynamic cutoff frequency of around 70 GHz.

The more important parameter for the varactor is its sensitivity, which is defined by  $S = (dC/C)(V/dV)$ . The sharp slope

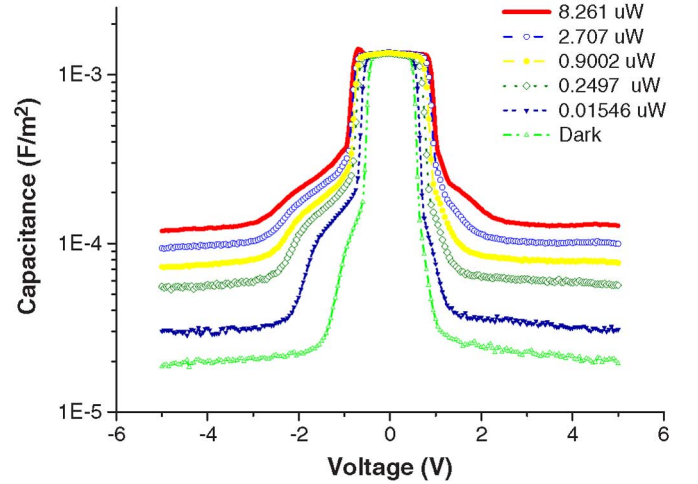


Fig. 3.  $C$ - $V$  characteristics under light at probe frequency of 10 kHz. The slopes of  $C$ - $V$  depend on the incident power levels.

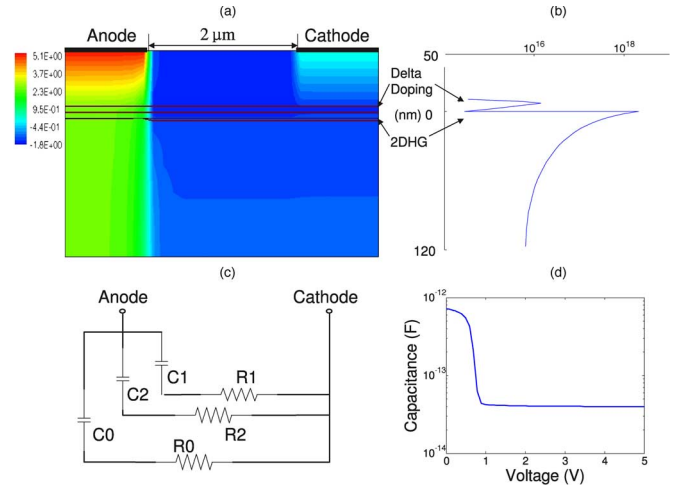


Fig. 4. (a) Simulated potential distribution at 5-V bias voltage. (b) Corresponding hole density at equilibrium. (c) Proposed circuit model, including  $C_0$ ,  $C_1$ , and  $C_2$ , representing contributions from background charge, delta-doping layer, and 2-D HG, respectively. (d) Simulated  $C$ - $V$  characteristics.

of the  $C$ - $V$ , as seen in Fig. 2, gives a sensitivity of 35, which to our knowledge is the highest reported. This high sensitivity based on the highly nonlinear  $C$ - $V$  relation is particularly suitable for high-order frequency-multiplication applications. The slope of the  $C$ - $V$  can be controlled by incident optical radiation. Fig. 3 shows the  $C$ - $V$  results under an 850-nm laser at various intensity values at a probe frequency of 10 kHz. Larger slopes are observed under lower intensities.

### III. DISCUSSION AND CONCLUSION

The device behavior was studied by simulation using integrated systems engineering (ISE)-technology computer-aided design (TCAD). Fig. 4(a) shows a 2-D potential distribution of the cross section of the device at a bias voltage of 5 V. As shown in the figure, most of the voltage drops at the reversed biased anode, with the depletion region extending vertically. The corresponding hole concentration along the growth direction cut in the middle of the device is shown in Fig. 4(b);

the two peaks represent the  $\delta$ -doping and 2-DHG, respectively. The charges underneath the anode are depleted under a bias of 5 V. In previous similar structure varactors [8], the  $C$ - $V$  behavior was modeled as parallel plate capacitors. In this case, all components of the capacitance due to the more complicated charge distributions should be considered. These consist of  $C_0$ ,  $C_1$ , and  $C_2$ , which are modeled as Fig. 4(c), representing the capacitance due to the background charge in the bulk, the mobile charge in 2-DHG, and the undepleted charge in  $\delta$ -doped layers, respectively. The background charge can include the bulk unintentional doping and the photogenerated carriers in the bulk absorption region. Under no bias, the capacitance is at maximum due to the combination of these three stored charge sources. With bias, it remains constant until the charges underneath the anode are depleted vertically. This regime corresponds to the flat peak in the  $C$ - $V$  characteristics. With further increase of the bias, as Fig. 4(a) shows,  $\delta$ -doping and 2-DHG charge start to be depleted laterally by a small Debye length, which make extremely small contributes to the total capacitance. In this regime  $C_0$ , the contribution from the background charge becomes dominant, which determines the slope of transition. In our device, the small bulk region possesses less background charge, resulting in a high sensitivity of the device. The difficulty in the lateral depletion of the 2-DHG causes a sudden drop of  $C_2$ , which also accounts for this high sensitivity.

Fig. 4(d) shows the simulated small signal  $C$ - $V$  at a frequency of 10 kHz. The difference between the  $C_{\max}$  from the simulated results and the measurement results is accounted for by the electrode pad capacitance. Our simulations also indicate that the shape of  $C$ - $V$  can be engineered by the charge distribution between the  $\delta$ -doping layer and the 2-D gas.

Under illumination, photogenerated carries create more background charge, which essentially changes the charge-distribution profile in the bulk, hence the voltage-dependent charge variations, namely, the  $C$ - $V$  characteristics. As shown in Fig. 3, the sensitivity of the varactor can be controlled by illumination. More importantly, since this is a photodetector device, it allows for interaction of optical and microwave signals. The extra background charge due to photogeneration, contributing to  $C_0$ , alleviates the steep drop of the capacitance. This explains the previous optical power modulated  $C$ - $V$  behavior.

In conclusion, we have fabricated an MSM-2-DHG heterostructure varactor capable of monolithic integration with III-V technology. The device demonstrates an excellent  $C_{\max}/C_{\min}$  ratio of up to 113 and extremely high sensitivity of up to 35, making it a good candidate for use in high-frequency-multiplier design. Alternately, optical intensity modulated sensitivity allows for the potential of applications in optoelectronic mixing. We have proposed a model for the observed device behavior accounting for the source of capacitance, including the contributions from the  $\delta$ -doping layer, 2-D gas, and background charge. The same principles can be applied to the design of a 2-DEG device.

## REFERENCES

- [1] P. Penfield and R. P. Rafuse, *Varactor Applications*. Cambridge, MA: MIT Press, 1962.
- [2] J. Maget, M. Tiebout, and R. Kraus, "Influence of novel MOS varactors on the performance of a fully integrated UMTS VCO standard 0.25- $\mu\text{m}$  CMOS technology," *IEEE J. Solid-State Circuits*, vol. 37, no. 7, pp. 953–958, Jul. 2002.
- [3] G. Chattopadhyay, E. Schlecht, J. S. Ward, J. J. Gill, H. H. S. Javadi, F. Maiwald, and I. Mehdi, "An all-solid-state broad-band frequency multiplier chain at 1500 GHz," *IEEE Trans. Microw. Theory Tech.*, vol. 52, no. 5, pp. 1538–1547, May 2004.
- [4] E. L. Kollberg and A. Rydberg, "Quantum-barrier-varactor diode for high efficiency millimeter-wave multipliers," *Electron. Lett.*, vol. 25, no. 25, pp. 1696–1697, Dec. 1989.
- [5] J. Vukusic, B. Alderman, T. A. Emadi, M. Sadeghi, A. Ø Olsen, T. Bryllert, and J. Stake, "HBV Tripler with 21% efficiency at 102 GHz," *Electron. Lett.*, vol. 42, no. 6, pp. 355–356, Mar. 2006.
- [6] R. Meola, J. Freyer, and M. Claassen, "Improved frequency tripler with intergrated single-barrier varactor," *Electron. Lett.*, vol. 36, no. 9, pp. 803–804, Apr. 2000.
- [7] Q. Xiao, Y. Duan, J. L. Hesler, T. W. Crowe, and R. M. Weikle, "A 5-mW and 5% efficiency 210 GHz InP-based heterostructure barrier varactor quintupler," *IEEE Microw. Wireless Compon. Lett.*, vol. 14, no. 4, pp. 159–161, Apr. 2004.
- [8] M. Marso, M. Wolter, P. Javarka, A. Fox, and P. Kordos, "AlGaIn/GaN varactor diode for integration in HEMT circuits," *Electron. Lett.*, vol. 37, no. 24, pp. 1476–1478, Nov. 2001.
- [9] A. Anwar, B. Nabat, and J. Culp, "An electrically and optically gate-controlled Schottky/2DEG varactor," *IEEE Electron Device Lett.*, vol. 21, no. 10, pp. 473–475, Oct. 2000.
- [10] M. Schefer, U. Lott, H. Benedickter, B. U. Klepser, W. Patrick, and W. Bachtold, "Monolithic coplanar, varactor tunable V-band HEMT oscillators with injection locking capability," *Electron. Lett.*, vol. 32, no. 20, pp. 1899–1900, Sep. 1996.
- [11] W. I. Wang, E. E. Mendez, and F. Stern, "High mobility hole gas and valence-band offset in modulation-doped p-AlGaAs/GaAs heterojunctions," *Appl. Phys. Lett.*, vol. 45, no. 6, pp. 639–641, Sep. 1984.